

Effects of plasma treatment in the tungsten process for chemical vapor deposition titanium nitride barrier film beyond nanometer technology

K.W. Chen^a, Y.L. Wang^{b,*}, L. Chang^a, F.Y. Li^c, G.J. Hwang^b

^aDepartment of Material Science and Engineering, National Chiao-Tung University, Hsin-Chu, Taiwan, ROC

^bCollege of Science and Engineering, National University of Tainan, Taiwan, ROC

^cDepartment of Chemistry, National Chung-Hsing University, Taichung, Taiwan, ROC

Available online 19 August 2005

Abstract

As the device shrunk to 100 nm, the CVD TiN barrier filling would be limited by the process window of contact for both step coverage and plasma treatment. This limitation not only affects the step coverage capability but also poses a challenge to the treatment of the organic film with the small contact hole. In this study, we investigated whether the plasma treatment of the TiN film barrier influences the subsequent tungsten deposition and causes the change of the gapfilling behavior. After the different RF plasma treatment, we found that the resistivity and impurity level of the thin TiN film can influence not only the contact resistance and uniformity, but also the product yield. The over-treatment contacts were found with porous voids in the poor tungsten deposition during the contact filling even after CMP polishing. The resistances of under-treatment contacts would be determined by the impurity level of TiN films. Hence, the optimized TiN deposition and treatment would be critical to the contact resistance and yield performance.

© 2005 Elsevier B.V. All rights reserved.

Keywords: CVD TiN; Tungsten; Barrier layer; Plasma treatment

1. Introduction

As the dimensions of devices shrink rapidly, the requirements of metallization become more critical. For contact VIA filling, the metallization process mostly applies with convectional chemical vapor deposition (CVD) method, even though copper physical vapor deposition (PVD) and electroplating technologies are applied widely in the back-end of line (BEOL) flow for interconnection metallization [1–6]. These CVD processes are included with the barrier metal of CVD TiN and plug-filling metal of W CVD. These methods demonstrate good capability of conformal gap-filling and low resistance in contact VIA integration and are widely adopted in the technologies below 130 nm. Besides, the convectional CVD method can remove several integration issues, such as metal spiking into the front end of line

(FEOL) device and high resistance of the contact issue if copper and tantalum barrier metal are introduced beyond 130 nm technology. However, the metallization processes of CVD face the challenges not only in the step coverage as the VIA size shrunk beyond 100 nm technologies, but also in the microstructure changes of TiN barrier and tungsten plug metal in a very narrow VIA which becomes more important for the overall VIA performance. For example, the CVD TiN process is applied with plasma treatment to reduce the impurity level, because the metallic organic compounds (such as tetrakis-dimethyl-amino-titanium, TDMAT, applied in the process reported in this paper) include lots of carbon and oxygen sources. The plasma treatment is generally recommended coupled with N₂/H₂ treatment and to achieve lower resistivity for CVD TiN film [2,7,8]. The treatment efficiency directly contributes to the changes in film resistivity, orientation, adhesion, and grain size [2,3]. These changes not only become more critical for VIA filling and resistance, but also make the influences on the quality of tungsten film, and even change the seam formation in the

* Corresponding author. Tel.: +886 6 5051400x5069; fax: +886 36 5051273.

E-mail address: ylwang@tsmc.com (Y.L. Wang).

small contact VIA size. For WCVD, the seam formation is accompanied with the subsequent nucleation and bulk deposition process on different VIA sidewalls [9]. But the seam formation beyond 100 nm technology is dependent on the VIA size and becomes critical in the VIA resistance and the quality of VIA gapfilling. Furthermore, as the aspect ratio of the contact VIA increases with the VIA size shrinks, the plasma treatment through high aspect ratio of VIA would change the treatment efficiency and film microstructure, and then affect the tungsten gapfilling or seam formation in VIA [1,10,11].

In general, the under-treatment barrier of CVD TiN makes the overall VIA resistivity increase from VIA barrier. Meanwhile, the over-treatment changes the properties of the TiN film and even tungsten film [1,8]. Not many reports available in literature discuss the integration issue for VIA metallization and optimization as the VIA size shrinks. In this paper, we investigated the effect of the underlying barrier of CVD TiN on the characteristics of the subsequent tungsten deposition, such as the orientation, resistivity, and gapfilling capability. Besides, we also discuss the effect on different treatment power and efficiency inducing the gapfilling capability of W CVD, and the change on the resistance and morphology of the contact VIA.

2. Experiment

Samples were prepared for the 100 nm contact VIA consisting of ion metal plasma titanium (IMP Ti) as the glue layer and CVD TiN as a barrier and adhesion layer, and the subsequent tungsten deposition as the contact plug filling. The IMP Ti and CVD TiN processes were integrated onto the 300 mm Applied Materials™ Endura and TxZ system, where IMP Ti utilized an inductively plasma (density around $10^{11-12}/\text{cm}^3$) to ionize the sputtered titanium metal atoms and then accelerated them across the sheath which was capacitively coupled with the additional radio frequency (RF) power to the substrate pedestal; and CVD TiN was introduced by reacting the metalorganic precursor, TDMAT, which was carried by He gas, in CVD system. The CVD system is operated in the chamber with the gas filling showerhead and the heating-coil susceptor, which are also capacitively coupled with a low frequency RF generator. Besides, the chamber is controlled with deposition rate as 7–10 Å/s, deposition temperature as 350–400 °C and operation pressure as 5–10 Torr. For the film preparation, the in-situ plasma treatment with N_2/H_2 mixing gas is consequentially required after the thermal TiN film deposition step [13,17]. A duration is defined by the combining the procedure of forming CVD TiN film with those of necessary depositions and the in-situ plasma treatment in CVD chambers. If the duration of 30 Å film depositions was repeated twice subsequently within one process, for example, we noted 2×30 Å as a total TiN film thickness of 60 Å. The in-situ plasma treatment in TiN film was

controlled by two major parameters, i.e., treated power and treated time. Besides, WCVD film on the barrier layers was prepared by the reaction of tungsten fluoride (WF_6), silane (SiH_4), and hydrogen (H_2) in the Applied Materials™ Centura system. For tungsten deposition, it is conducted at the temperature range of 400–425 °C in a single wafer reactor. WF_6/SiH_4 ratio variation is controlled for plug-filling completion [9]. By adjusting above two CVD TiN parameters, plasma treatment power and treated time, we analyzed the effects of the tungsten film on the grain size and orientation. The analysis methods included Auger electron spectroscopy (AES) for film composition, the four-point probe for film resistivity, X-ray diffraction (XRD) for film orientation, and scanning electron microscopy (SEM) for surface microstructure. The gapfilling capability was observed by the cross-sectional transmission electron microscopy (TEM).

3. Results and discussion

As shown in Fig. 1, the film resistivity change strongly depended on the deposition time under the same treatment conditions. The relation between resistivity and deposition time could be roughly divided into two regions, i.e., less and more than 16.5 s of the deposition time. In the first region, the resistivity decreased as the deposition time increased, while in the other region, the resistivity increased along with the increase of the deposition time. The observation found in the second region was corresponding to the concentration increase in organic impurity with the increase in the deposition thickness of CVD TiN. The different characteristics found in the first region were due to the over-treatment phenomena occurred on the film, i.e., the high energy treatment not only made most of the organic impurity disappeared in the film, but also led to the grain growth, orientation change, and compactness in the film structure [10–12]. Hence, the “over-treatment” phenomenon can be defined as the resistivity increasing but with the most compact thickness achieved while the plasma treatment energy kept increasing, due to the film property change such as the phase and grain growth. In Table 1, it demonstrated the effects of various treated powers on the film resistivity and thickness under the different durations of CVD TiN deposition and treatment. On the first condition, the film resistivity increased as the treated power increased when the overall TiN thickness remained almost the same. Similar to the first region in Fig. 1, the grain growth and orientation played an important role in the over-treatment conditions. In the 2nd or 3rd conditions of Table 1, the film resistivity decreased as the treated power increased. However, in the 2nd condition, not only the film thickness could be kept almost the same, but also the impurity could be removed out of the film, which is in its most compact structure. Meanwhile, in the 3rd condition, the similar trends were found as in the 2nd condition, i.e., the impurity decrease and

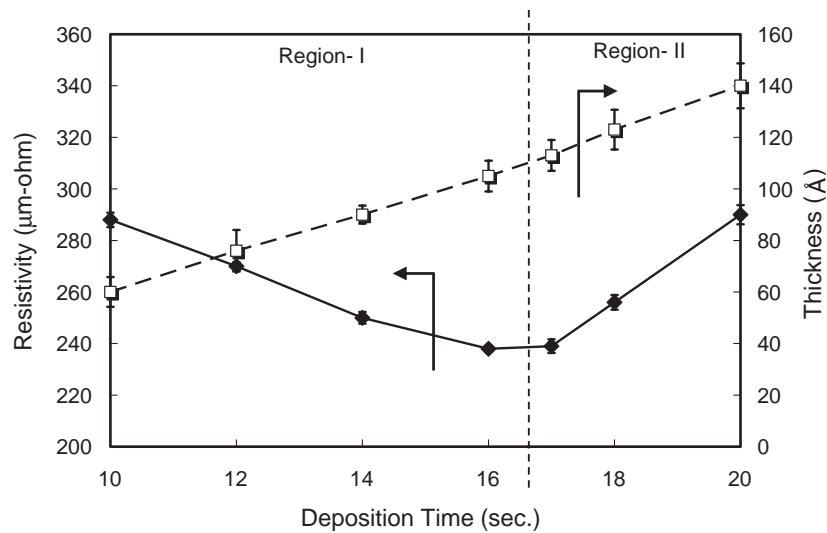


Fig. 1. The relationship between CVD TiN deposition time and the film resistivity and thickness with the plasma treatment with energy under 0.01 kW h (or equal to 0.01 kW h).

formation of the compact film structure, but the film thickness decreased as the treated power increased. To sum up the experimental mechanisms of the condition (2) and (3) in Table 1, the grain growth would be inferred and induced by the energy of the treated power, and then the grain boundary and the impurity concentration were reduced and contributed to the lower resistivity until the most compact structure of the film was achieved with enough treated powers [12–14]. From the result of condition (1) in Table 1, the film orientation change could be triggered by the over-treated power.

3.1. The change of tungsten phase due to the underlying TiN layer

The tungsten phase distribution is known to strongly follow the underlying layer structure [10]. Therefore, any physical change for underlying TiN layer would directly reflect in the phase distribution of tungsten film. Fig. 2(a) showed the major orientation distribution of tungsten film deposited subsequently on TiN film would be changed as the treated power increased. With the similar reason, the orientation of the tungsten film also tended to form the (110) phase as the treated time increased. Tungsten films often exhibit bcc crystal structure and their diffraction patterns

shall contain (110), (200), and (211); but the (110) phase for tungsten was corresponding to the lowest interface energy on these TiN films, which is, in turn the minimum-energy structure [10,15,16]. This was the reason that the treated energy, i.e., the product of the treated power and time, could change the TiN film orientation under the over-treatment condition, and then affect the tungsten orientation. Besides, the IMP Ti thickness under CVD TiN film could influence indirectly on the tungsten film orientation, as shown in the Fig. 2(b). It was because the thickness of the bottom IMP Ti film created the different initial nucleation stage for CVD TiN, and then affected the tungsten film deposited subsequently [17]. Much thicker IMP Ti film would increase the intensity of tungsten (110) phase. However, the contact VIA shrinkage is not compatible with the thicker IMP Ti film or over-treatment condition on the CVD TiN film, due to higher resistivity performed on the VIA, which even affected the growth filling of the tungsten film on the VIA hole. Fig. 3 showed the intensity of the tungsten (110) phase and its grain size on the previous different treatments of CVD TiN film. From the experimental results, the intensity of the tungsten film with (110) phase was strongly dependent on the treatment energy of the previous layer CVD TiN. Noticeably, the intensity of the tungsten film with (110) phase would not increase as the treatment energy over 0.018

Table 1
Effect of different power treatments on the properties of the deposited TiN films

Condition	(1) TiN dep. 5 s, treatment 20 s (duration 4 times)			(2) TiN dep. 10 s, treatment 20 s (duration 2 times)			(3) TiN dep. 20 s, treatment 20 s (duration 2 times)		
	Sheet Resist., Rs (Ω /sq)	Thickness (nm)	Resistivity ($\mu\Omega$ cm)	Sheet Resist., Rs (Ω /sq)	Thickness (nm)	Resistivity ($\mu\Omega$ cm)	Sheet Resist., Rs (Ω /sq)	Thickness (nm)	Resistivity ($\mu\Omega$ cm)
1350	422.8	87.7	369.8	206.6	147.6	304.8	206.9	184.5	381.6
1550	426.0	88.0	373.5	197.8	147.9	292.3	194.9	182.9	356.7
1750	433.7	87.4	377.6	190.3	145.3	276.2	182.4	181.3	330.9
Trend	↑		↑	↓		↓	↓	↓	↓

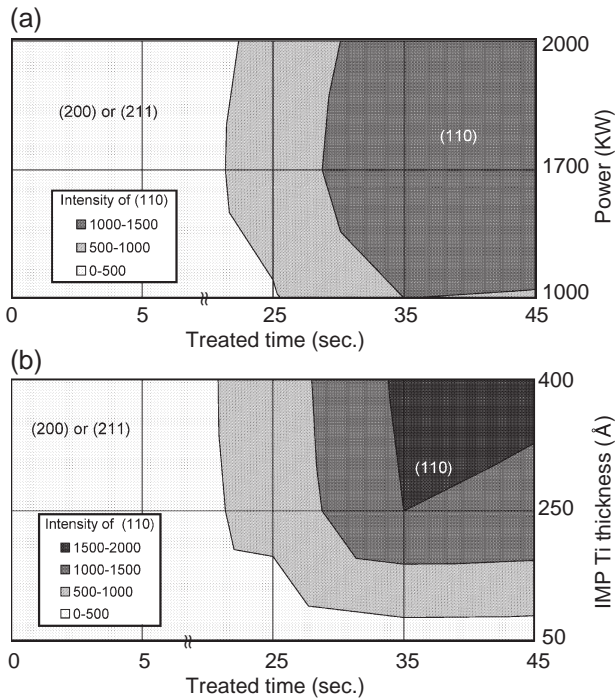


Fig. 2. Comparison between the changes of the tungsten phase under (a) different CVD TiN treated power and time; and (b) different IMP Ti thickness and CVD TiN plasma treated time.

kW h. Under this condition, the tungsten grain size reached the maximum size. While this size of tungsten filled into the VIA hole, the gapfill capability would be not very high, and accompanied with much more grain boundaries and void in the VIA hole. In the other words, this grain size distribution would reduce the gapfill quality of tungsten, and even enhance the seam formation. However, judging from Table 1, the over-treatment condition would increase the resistivity of the CVD TiN film and even the tungsten grain size (while the corresponding energy is over 0.018 kW h), but the thickness of the film was kept roughly constant.

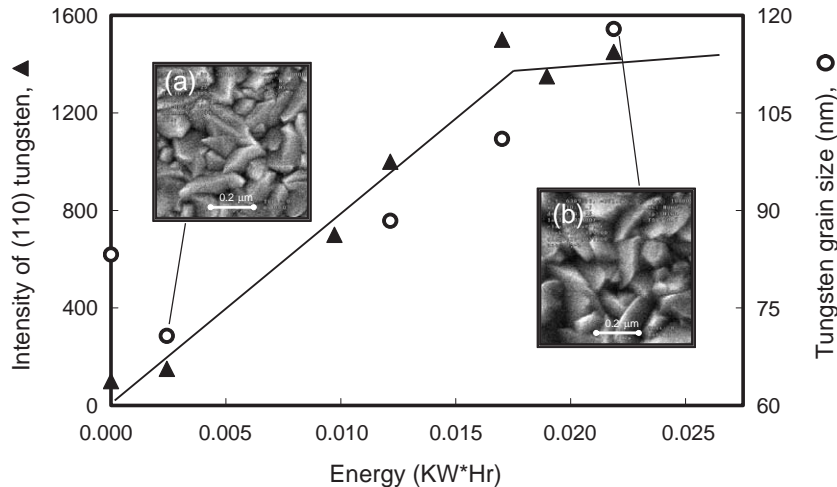


Fig. 3. The effect of the CVD TiN treated energy on the phase intensity and grain size distribution of tungsten (110).

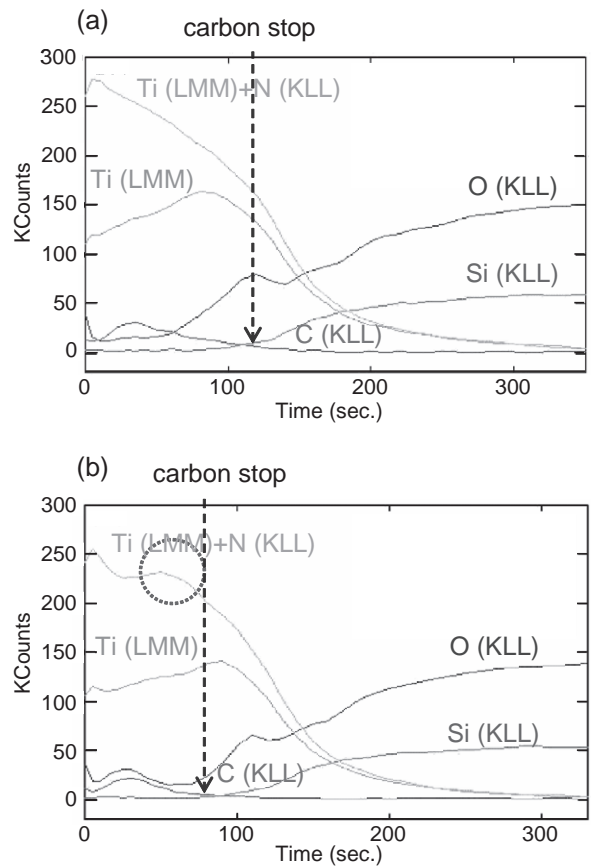


Fig. 4. AES analysis for the 2x30 Å CVD TiN film under (a) the normal treatment condition, i.e., the plasma treated energy under 0.010 kW h; and (b) the over-treatment condition, i.e., plasma treated energy over 0.020 kW h.

3.2. Over-treatment mechanism from blanket wafer

Fig. 4 showed the atomic depth profile across the CVD TiN film deposited on IMP Ti with different power treatments. Fig. 4(a) was with the treatment of the 0.0075 kW h energy, while Fig. 4(b) was over 0.02 kW h energy.

As shown in the Fig. 4, one of Ti (LMM) signals overlaid with N (KLL), which was designated as “Ti (LMM)+N (KLL)”. It was observed clearly that the signal of “Ti (LMM)+N (KLL)” had a protuberant profile near the interface of Ti/TiN and that of “Ti (LMM)” kept at the similar level after plasma treatment. It indicated that the nitrogen would become richer in the interface after plasma treatment with higher energy was applied, as shown in Fig. 4(b); that is, the higher treated energy could force the nitrogen penetrating into the underlying IMP Ti layer, and subsequently change the interface behavior between IMP Ti and CVD TiN films. The interface was indicated as the sign of the “carbon stop” of Fig. 4. Besides, the carbon stop means that the inorganic components disappear in the film of CVD TiN from the plasma treatment. Compared with the signals of the carbon stop for both cases of Fig. 4, the condition of Fig. 4(b) corresponded to the lower impurity concentration due to the CVD TiN deposition from TDMAT chemical with high carbon source. It implied that the high treatment energy could eliminate the carbon content or impurity concentration of the CVD TiN film.

3.3. Over-treatment applied to contact VIA for pattern wafer

To observe the over-treatment effect on the gapfill or resistance of the contact VIA, the different plasma powers were applied to the contact VIA with the higher aspect ratio (>5) and 110 nm width of contact hole. The results, shown in Fig. 5, indicated that the treatment, with energy higher than 0.02 kW h, induced the distribution of resistance probability with longer tailing. Employing TEM analysis to the high resistance of contact VIA with the treated energy over 0.02 kW h as applied in the condition of Fig. 5, we found that the poor formation of tungsten fill into the contact hole was similar to the volcano phenomena, which

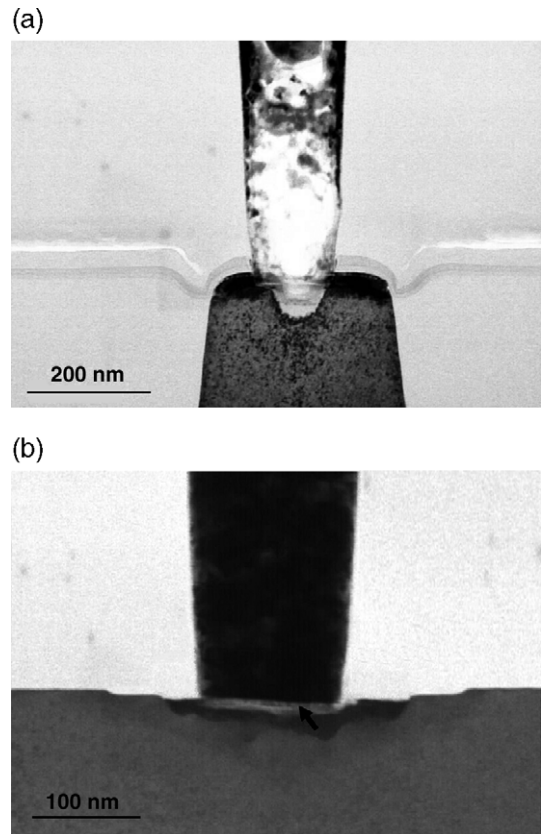


Fig. 6. TEM pictures of high resistance on the contact for different over-treatment conditions for the $2 \times 30 \text{ \AA}$ CVD TiN film; (a) plasma treated energy over 0.015 kW h; (b) plasma treated energy over 0.02 kW h.

exposed the tungsten and contact hole, as shown in Fig. 6(a) [1,15,18–20]. In addition, while the treated energy reduced to the level of 0.015 kW h, the over-treatment applied to the VIA with nitrified IMP Ti film caused the CVD TiN film

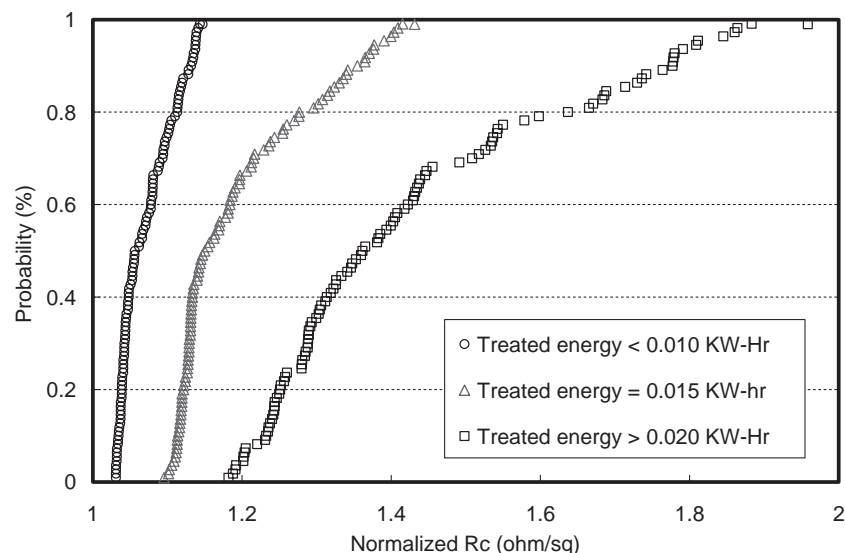


Fig. 5. The distribution of contact resistance under different CVD TiN plasma treatment energies.

formed underneath the VIA bottom, as shown in Fig. 6(b). It also implied that the high energy makes nitrogen penetrate deep into TiN film and react with IMP Ti to form TiN film. However, the TiN film, with the treated energy over 0.02 kW h, would make the resistance and uniformity of VIA increased, as shown in the Fig. 5. In spite of the tungsten seam hole which was not shown in Fig. 6(b), the nitrified IMP Ti film was responsible for the effect of the thinner pure Ti film on the (200) phase of tungsten, which preferred to filling into the contact. Although the contact seemed to be shrink to free seam size and reduce the contact resistance during seam formation, the nitrified IMP Ti films still increased to the overall contact resistance, which could be contributed by the resistance of tungsten, CVD TiN, and IMP Ti films filled in the contact. Based on the above summarization, when the energy was over 0.02 kW h, the fully nitrified IMP Ti or over-penetrated VIA bottom with the damage substrate below the contact would affect the tungsten formation in the contact hole. Tungsten of CVD deposition was reacted with SiH₄, H₂, and WF₆, and then produced the residue gas HF diffused out of the contact. But the HF gas could react with Ti film to form TiF₃ compounds which, in turn, exposed to the contact. Hence, the over-treatment for CVD TiN with the condition of the treated energy over 0.02 kW h would cause the poor formation of tungsten in the contact VIA, as shown in Fig. 6(a).

4. Conclusions

Plasma treatment induced the different changes of the CVD TiN film from high resistivity for under-treatment condition to low resistivity coupled with phase change for over-treatment condition. The subsequent tungsten deposition followed the pattern of the underlying TiN layer to influence the film phase, grain size, and nucleation, which all in turn affected the tungsten gapfill capability. Through the verification by TEM, the over-treatment implemented in 110 nm contact VIA would make the nitrified IMP-Ti glue layer below the contact bottom, and even penetrate and damage the contact bottom to form the volcano effect on the tungsten plug filling.

Acknowledgements

This work was supported by the National Science Council, Taiwan, R.O.C. (Project No. NSC92-2113-M-260-005).

References

- [1] P.J. Ireland, *Thin Solid Films* 304 (1997) 1.
- [2] R. Kroger, M. Eizenberg, C. Marcadal, L. Chen, *J. Appl. Phys.* 91 (2002) 5149.
- [3] S. Ikeda, J. Palleau, J. Torres, B. Chenevier, N. Bourhila, R. Madar, *J. Appl. Phys.* 86 (1999) 2300.
- [4] J.Y. Yun, S.W. Rhee, *Thin Solid Films* 312 (1998) 24.
- [5] S.L. Zhang, R. Palmans, J. Keinonen, C.S. Petersson, K. Maex, *Appl. Phys. Lett.* 67 (1995) 2998.
- [6] M. Biberger, S. Jackson, G. Tkach, J. Schlueter, B. Jones, C.K. Huang, Luc Ouellet, *Thin Solid Films* 270 (1995) 522.
- [7] B.K. Lim, H.S. Park, A.K.H. See, E.Z. Liu, S.H. Wu, *J. Vac. Sci. Technol., B* 20 (6) (2002) 2219.
- [8] M. Daneek, M. Liao, J. Tseng, K. Littau, D. Saigal, H. Zhang, R. Mosely, M. Eizenberg, *Appl. Phys. Lett.* 68 (1996) 1015.
- [9] J. Wu, Y.L. Wang, J. Dun, Y.L. Wu, H. Zhang, A. Wang, *J. Vac. Sci. Technol., B* 17 (5) (1999) 2300.
- [10] Y.C. Peng, L.J. Chen, W.Y. Hsieh, Y.R. Yang, Y.F. Hsieh, *Solid-State and Integrated Circuit Technology, USA*, 21–23 Oct., 1998. Proceedings, 1998 5th International Conference on, 1998, p. 211.
- [11] C.M. Yu, M.Y. Wang, S.L. Shue, C.H. Yu, M.S. Liang, *VLSI Technology, Systems, and Applications, USA*, 18–20 April, 2001. Proceedings of Technical Papers, 2001 International Symposium on, 2001, p. 261.
- [12] J.M. Bulger, C.S. Whelan, A. Dumont, M. Kuhn, J. Clark, *J. Vac. Sci. Technol., B* 17 (2) (1999) 410.
- [13] J.K. Lan, Y.L. Wang, C.G. Chao, K.Y. Lo, Y.L. Cheng, *J. Vac. Sci. Technol., B* 21 (4) (2003) 1224.
- [14] D.H. Kim, G.T. Lim, S.K. Kim, J.W. Park, J.G. Lee, *J. Vac. Sci. Technol., B* 17 (5) (1999) 2197.
- [15] J.H. Je, D.Y. Noh, H.K. Kim, K.S. Liang, *J. Appl. Phys.* 81 (1997) 6126.
- [16] A.C. Westerheim, J.M. Bulger, C.S. Whelan, T.S. Sriram, L.J. Elliott, J.J. Maziarz, *J. Vac. Sci. Technol., B* 16 (5) (1998) 2729.
- [17] J.K. Lan, Y.L. Wang, K.Y. Lo, C.P. Liu, C.W. Liu, J.K. Wang, Y.L. Cheng, C.G. Chau, *Thin Solid Films* 398–399 (2001) 544.
- [18] A. Mouroux, S.L. Zhang, C.S. Petersson, R. Palmans, K. Maex, T. Ahlgren, *Surf. Coat. Technol.* 99 (1998) 274.
- [19] L. Ulmer, L. George, J.C. Veler, Y. Morand, M. Bakli, V. Ferrier, M. Lerme, L. Perroud, T. Morel, *Microelectron. Eng.* 33 (1997) 121.
- [20] Y.C. Peng, L.J. Chen, W.Y. Hsieh, Y.R. Yang, Y.F. Hsieh, *J. Vac. Sci. Technol., B* 16 (4) (1998) 2013.